

Conductivity sum rules and energy scales in high-temperature superconductors

C. C. Homes and S. V. Dordevic

Department of Physics, Brookhaven National Laboratory, Upton, New York 11973

D. A. Bonn, Ruixing Liang, and W. N. Hardy

Department of Physics and Astronomy, University of British Columbia, Vancouver, British Columbia, Canada V6T 1Z1

(Dated: January 29, 2019)

The Ferrell-Glover-Tinkham (FGT) sum rule has been applied to the temperature dependence of the optical conductivity of optimally-doped $\text{YBa}_2\text{Cu}_3\text{O}_{6.95}$ and underdoped $\text{YBa}_2\text{Cu}_3\text{O}_{6.60}$ for light polarized along the a axis. While the sum rule is obeyed in both materials, the energy scale ω_c required to recover the full strength of the superuid ω_s is dramatically different; $\omega_c \approx 800 \text{ cm}^{-1}$ in the optimally doped system (close to the maximum of the superconducting gap, 2Δ), but $\omega_c \approx 5000 \text{ cm}^{-1}$ in the underdoped system. While the normal-state scattering rate determines the energy scale just above the critical temperature ($T > T_c$), in the superconducting state the relevant energy scale for ω_s should be $\approx 2\Delta$, with little sensitivity to T . In both systems, $\omega_s < 2\Delta$, reinforcing this view. The preservation of the FGT sum rule in the optimally-doped materials suggests that within the accuracy of this measurement the majority of the spectral weight of the condensate comes from $\omega < 2\Delta$ and is therefore related to potential rather than kinetic energy changes. In the underdoped material the distinction between potential and kinetic energy is not as clear. The fact that the FGT sum rule is preserved does not rule out a kinetic energy contribution to ω_s . The different behavior of these two materials suggests that the nature of the normal state plays a deciding role in the nature of the superconductivity.

PACS numbers: 74.25.-q, 74.25.Gz, 78.30.-j

I. INTRODUCTION

Sum rules and conservation laws play an important role in physics. In spectroscopy, the conductivity sum rule is particularly useful and is an expression of the conservation of charge.¹ In metallic systems, the conductivity sum rule usually yields the classical plasma frequency. In superconductors, below the critical temperature T_c some fraction of the carriers collapse into the δ -function at zero frequency that determines the London penetration depth

λ_L , with a commensurate loss of spectral weight from low frequencies (below twice the superconducting energy gap). This shift in spectral weight may be quantified by another sum rule as discussed by Ferrell, Glover and Tinkham (the FGT sum rule).^{2,3} The theory of superconductivity described by Bardeen, Cooper and Schrieffer (BCS)⁴ holds that while the kinetic energy of the superconducting state is greater than that of the normal state,⁵ this increase is compensated by the reduction in potential energy which drives the transition.⁶ However, it has been proposed that in certain hole-doped materials the superconductivity could arise from a lowering of the kinetic rather than the potential energy.⁷ In such a system, the FGT sum rule would appear to be violated and would yield a value for the strength of the superconducting condensate $\omega_s = c^2/\lambda_L^2$ that would be too small (λ_L would be too large). In addition, this would be accompanied by a decrease in the spectral weight at frequencies much higher than the superconducting energy gap (i.e., non-local transfers of spectral weight).^{7,8,9} Similar models in the cuprate materials presume either strong coupling,^{10,11} or that the normal state is not a Fermi

liquid and that superconductivity is driven either by the recovery of frustrated kinetic energy when pairs are formed,^{12,13} by lowering the in-plane zero-point kinetic energy,¹⁴ or by the condensation of preformed pairs.¹⁵

Experimental results for the optical properties for light polarized along the interplane, or c axis direction in several different cuprate materials suggests that these predictions are realized and that the change in the low-frequency spectral weight accounts for only about half of the strength of the condensate in this direction.^{16,17,18} The apparent violation of the FGT sum rule is restricted to the underdoped materials¹⁸ which display a pseudogap in the c axis conductivity.^{19,20} The dramatically lower value of the strength of the condensate along the c axis makes it easier to observe kinetic energy contributions. However, the reduction of the kinetic energy is still far less than the condensation energy.²¹ If kinetic energy effects play a role in the condensation, then they must originate from the in-plane response, but because the in-plane kinetic energy is quite large, small changes at high frequency leading to violations of the sum rule may be difficult to detect.^{22,23} Within the limits of experimental accuracy, no violation of the FGT sum rule has been observed in previous studies of the in-plane optical properties.¹⁸ However, it has recently been reported that

0.3% of the total intraband spectral weight is removed from the high-frequency (near-infrared and visible) region at the onset of superconductivity,^{24,25,26} suggesting that observable changes in the kinetic energy are taking place.

In this paper we examine the changes of the in-plane spectral weight and the evolution of the superconducting condensate in the optimally doped and underdoped

$\text{YBa}_2\text{Cu}_3\text{O}_{6+x}$. The BCS model requires that the spectral weight of the condensate be fully formed at energies comparable to the energy gap (Δ), with no subsequent violation of the FGT sum rule. This is indeed observed for the optimally-doped system (within the limits of experimental accuracy, which is estimated to be better than 0.5%). The fact that this result is similar to that of a BCS system suggests that the condensation energy in this material is due to a potential energy mechanism. While the FGT sum rule is also preserved in the underdoped material, the full weight of the condensate is recovered only at much higher energy relative to the superconducting energy gap. However, the non-Fermi liquid nature of the normal state and the large energy scales observed for the condensate have led to the suggestion that the potential and kinetic energy may be mixed.²⁷ In such a case, the fact that the FGT sum rule is obeyed does not rule out the possibility of a contribution to the condensate from the kinetic energy.

II. EXPERIMENT AND SAMPLE PREPARATION

Details of the growth and characterization of the mechanically-detwinned $\text{YBa}_2\text{Cu}_3\text{O}_{6+x}$ crystals has been previously described in detail^{28,29} and will be discussed only briefly. The crystal had a small amount of Ni deliberately introduced, $\text{Cu}_{1-x}\text{Ni}_x$, where $x = 0.0075$. Such a small concentration of Ni results in a critical temperature which is slightly lower (2 K) and slightly broader than the pure materials. The same detwinned crystal has been carefully annealed to produce two different oxygen concentrations, $x = 0.95$ ($T_c = 91$ K) and 0.60 ($T_c = 57$ K). The resistance for light polarized along the a axis (perpendicular to the CuO chains, therefore probing the only the CuO₂ planes) has been measured over a wide frequency range at a variety of temperatures using an over-lying technique,³⁰ and the optical properties calculated from a Kramers-Kronig analysis. The optical conductivity, which dealt primarily with the effects of Ni doping on the CuO chains and the reduction of the in-plane anisotropy, has been previously reported.³¹ The presence of Ni in such small concentrations was not observed to have any effect on the conductivity of in the CuO₂ planes in either the normal or superconducting states.

III. RESULTS AND DISCUSSION

A. Optical sum rules

Optical sum rules comprise a powerful set of tools to study and characterize the lattice vibrations and electronic properties of solids. The spectral weight may be estimated by a partial sum rule of the conductivity^{1,32}

$$N(\omega_c) = \frac{120}{\pi} \int_0^{\omega_c} \frac{\sigma_1(\omega) d\omega}{\omega^2 - \omega_p^2} \quad (1)$$

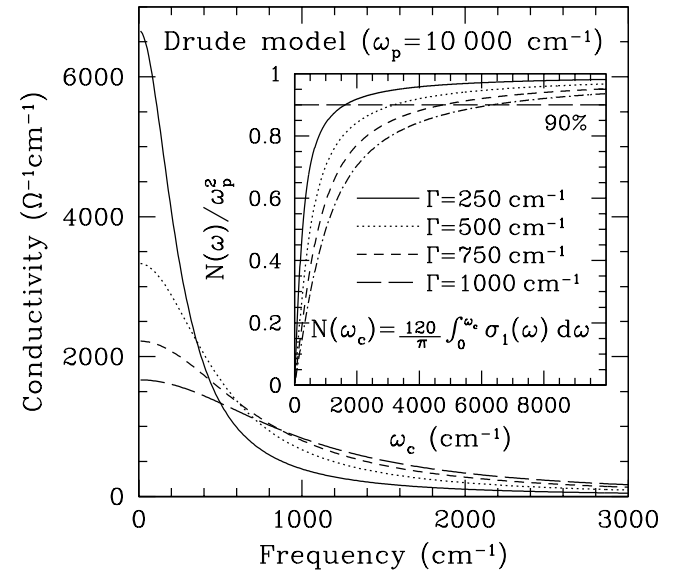


FIG. 1: The real part of the optical conductivity for the Drude model with $\omega_p = 10000 \text{ cm}^{-1}$ and several different scattering rates, $\Gamma = 250, 500, 750$ and 1000 cm^{-1} . The conductivity has the form of a Lorentzian centered at zero frequency, with a width of Γ . For large values of Γ , spectral weight is transferred from low to high frequency. Inset: The conductivity sum rule applied to the real part of the optical conductivity from the Drude model. The integral has been normalized to ω_p^2 and will approach unity at high frequency. The spectral weight captured by the integral increases quickly and has approached 90% of its full value about $\omega_c = 6800 \text{ cm}^{-1}$. For large values of Γ , the cut-off frequency can be larger than ω_p .

where $\omega_p^2 = 4ne^2/m$ is the classical plasma frequency, n is the carrier concentration, and m is an effective mass. In the absence of bound excitations, this expression is exact in the limit of $\omega_c \gg 1/\Gamma$, thus $N(\omega_c) \approx 1$ and the spectral weight is $N(\omega_c) \approx 1$. However, any realistic experiment involves choosing a low-frequency cut-off ω_c . In order to test what a reasonable choice for ω_c is, we consider the simple Drude model for the complex dielectric function $\epsilon = \epsilon_1 + i\epsilon_2$

$$\epsilon(\omega) = \epsilon_1 - \frac{\omega_p^2}{\omega(\omega + i\Gamma)}; \quad (2)$$

where ϵ_1 is the high frequency contribution to the dielectric function from the ionic cores, and $\Gamma = \Gamma_1 + \Gamma_2$ is the scattering rate. The optical conductivity $\sigma = \epsilon_1 + i\epsilon_2 = \epsilon_1/\omega$ is understood to have units of $\text{A}^2 \text{cm}^{-1}$. The real part of the conductivity is shown in Fig. 1 for $\omega_p = 10000 \text{ cm}^{-1}$ and several different choices for the scattering rate $\Gamma = 250, 500, 750, 1000 \text{ cm}^{-1}$; $\sigma(\omega)$ does not depend on the choice of ω_c . The conductivity can be described by a Lorentzian line shape centered at zero frequency, where Γ is the width at half maximum; as Γ increases, spectral weight is transferred from low to high frequencies.

The conductivity sum rule has been applied to the Druedahl model shown in Fig. 1 as a function of the cut-off frequency ω_c and normalized to ω_p^2 ; the evolution of the spectral weight is shown in the inset of this figure. The integral is denoted as $N(\omega)$, as the quantity is effectively integrating out the number of carriers in the system. As the full spectral weight is captured, $N(\omega) = \omega_p^2$ should approach unity. As the inset in Fig. 1 illustrates, the 90% threshold is achieved for $\omega_c \approx 6 - 8$, which indicates that the majority of the spectral weight associated with the free carriers in the Druedahl model lies within this region. It should be noted that even for relatively small values of Γ this introduces a broad interval, and that larger choices of Γ leads to values of ω_c that rival ω_p . This places some useful constraints on the conditions for the conductivity sum rule.

The conductivity in the superconducting state for any polarization r has two components⁵

$$\sigma_{1;r}^{SC}(\omega) = \sigma_{s;r}(0) + \sigma_{1;r}^{reg}(\omega); \quad (3)$$

The first part is associated with the superconducting function at zero frequency, where $\sigma_{s;r} = \sigma_{1;r}^2 = \frac{2}{\omega_p^2}$ is the superfluid stiffness or strength of the superconducting order (the critical temperature is a measure of the phase coherence of the system³³). This is often expressed as the square of a plasma frequency $\omega_{ps}^2 = 4 n_s e^2 / m_r$, where n_s is the density of superconducting electrons, and m_r is the effective mass tensor. The second component $\sigma_{1;r}^{reg}(\omega)$ is referred to as the 'regular' component for $\omega > 0$ and is associated with the unpaired charge carriers.

A variation of the conductivity sum rule in a superconductor is to study the amount of spectral weight that collapses into the superconducting function at the origin⁵ below the critical temperature T_c . This scenario is represented in Fig. 2, which shows the normalized conductivity for a BCS model for an arbitrary purity level³⁴ where the scattering rate in the normal state has examined for several different values, (a) $\Gamma = 2$, (b) $\Gamma = 2$ and (c) $\Gamma = 10$, where Δ is the full value for the superconducting energy gap for $T = T_c$. The solid line shows the real part of the optical conductivity $\sigma_1(\omega)$ in the normal state for $T > T_c$, while the dashed line is the calculated value for $\sigma_1(\omega)$ in the superconducting state for $T = T_c$. For $T = T_c$ the gap is fully formed, and there is no conductivity for $\omega < \Delta$, above which the onset of absorption occurs. In Fig. 2(a) the majority of the normal-state spectral weight lies below Δ and will collapse into the condensate; this is essentially the 'clean limit' case. In Fig. 2(b) the scattering rate is larger and a considerable amount of spectral weight now lies above Δ . Finally, Fig. 2(c) illustrates a 'dirty-limit' case where most of the spectral weight lies above Δ .

The missing spectral weight represented by the hatched area represents the strength of the condensate

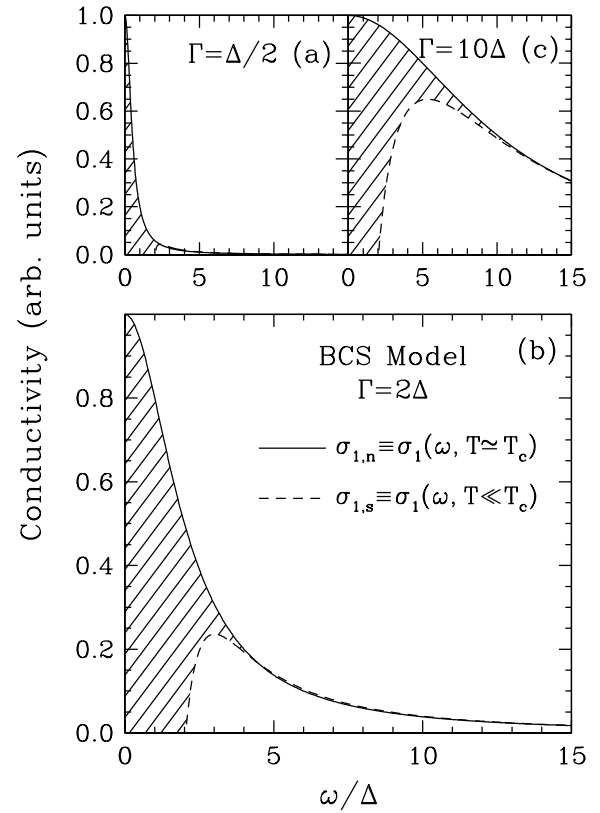


FIG. 2: The real part of the optical conductivity calculated for a BCS model with an arbitrary level of impurities for several different normal-state scattering rates; (a) $\Gamma = 2$, (b) $\Gamma = 2$, and (c) $\Gamma = 10$. The conductivity in the normal state $\sigma_1(\omega; T > T_c)$ is shown by the solid line (normalized to unity), while the conductivity in the superconducting state $\sigma_1(\omega; T = T_c)$ is shown by the dashed line. For $T = T_c$ the superconducting gap Δ is fully formed and there is no absorption in this region. The hatched area illustrates the spectral weight that has collapsed into the superconducting function at the origin. For small normal-state scattering rates shown in (a), much of the spectral weight lies below Δ and will collapse into the condensate. As the Γ increases in (b) and (c), more spectral weight is pushed out to frequencies above Δ and as a result the strength of the condensate will decrease.

ω_{ps}^2 . This area may be estimated by the sum rule

$$\omega_{ps}^2 = \frac{120}{\pi} \int_0^{\Delta} [\sigma_1(\omega; T > T_c) - \sigma_1(\omega; T = T_c)] d\omega; \quad (4)$$

This sum rule is referred to as the Ferrell-Glover-Tinkham sum rule.^{2,3} An alternative method for extracting the superfluid density relies on only the real part of the dielectric function (the imaginary part of the conductivity). If upon entering the superconducting state for $T = T_c$ it is assumed that all of the carriers collapse into the condensate, then $\omega_{ps} = \omega_p$ and $\epsilon = 0$, so that the form of the dielectric function in Eq. (2) becomes $\epsilon(\omega) = \sigma_1(\omega) = \sigma_1 \omega_p^2 = \omega_p^2$; in the limit of $\omega \ll \Delta$,

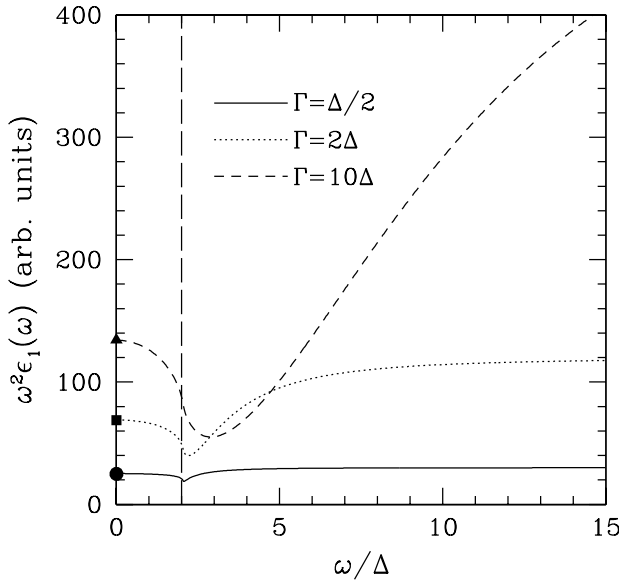


FIG. 3: The values of $\omega^2 \epsilon_1(\omega)$ calculated from the BCS model for $T = T_c$ for the three choices of normal-state scattering rate $\Gamma = \Delta/2$ (solid line), 2Δ (dotted line), and 10Δ (dashed line); $\omega_s = \omega^2 \epsilon_1(\omega)$ in the limit of $\Gamma \rightarrow 0$. Note that there is also a slight minimum near 2Δ (long dashed line) for the different choices of

$\omega_s / \omega_{ps}^2 = \omega^2 \epsilon_1(\omega)$. The value for $\omega^2 \epsilon_1(\omega)$ is shown in Fig. 3 for the three different choices of Γ that were shown in the previous figure. In each case there is a small dip near 2Δ , and the curves converge cleanly in the $\Gamma \rightarrow 0$ limit. The determination of ω_s from $\omega^2 \epsilon_1(\omega)$ has two main advantages: (i) it relies only on the value of $\epsilon_1(\omega)$ for $T = T_c$ and thus probes just the superfluid response, and (ii) ω_s is determined in a low-frequency limit, which removes the uncertainty of the high-frequency cut-off frequency ω_c in the FGT sum rule estimates of the condensate. We will distinguish between values of the condensate determined from $\omega^2 \epsilon_1(\omega)$ as ω_s , and the FGT sum rule as ω_{ps}^2 . The two techniques should in fact yield the same result, and it is indeed useful to compare the high-frequency estimates of ω_{ps}^2 with ω_s .

The rapidity with which the spectral weight of the condensate is captured by the Ferrell-Glover-Tinkham sum rule is shown in Fig. 4 for three different choices of the normal-state scattering rate relative to the superconducting energy gap. Here the solid line is the conductivity sum rule applied to $\epsilon_1(\omega)$ in the normal state ($T > T_c$), effectively ω_p^2 , while the dotted line is the conductivity sum rule for $T = T_c$, which yields $\omega_p^2 - \omega_{ps}^2$. The difference between the two curves is the dashed line, which is simply ω_{ps}^2 . To simplify matters, in each case the integrals have been normalized with respect to the strength of the fully-formed condensate ω_s , to yield a dimensionless ratio. In Fig. 4(a) the normal-state scattering rate has been chosen to be $\Gamma = 2\Delta$ ("clean limit"). It may

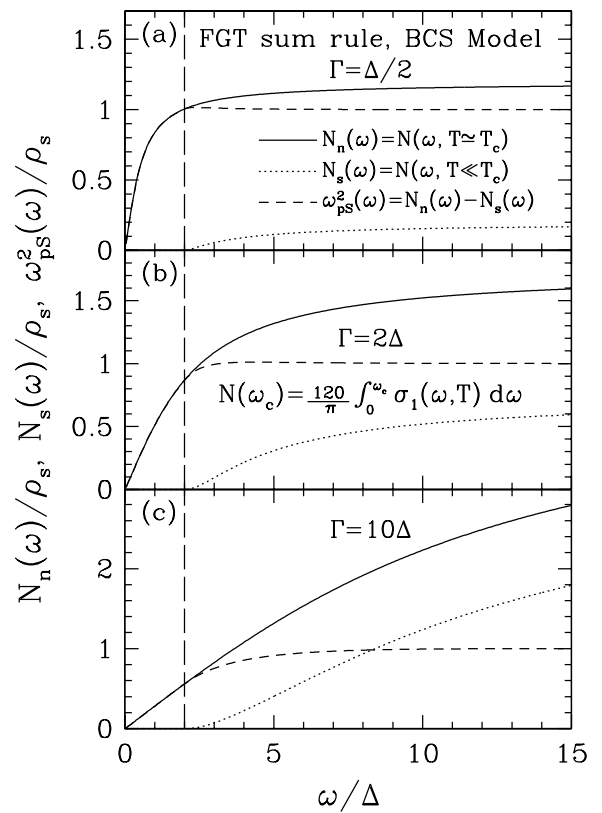


FIG. 4: The Ferrell-Glover-Tinkham (FGT) sum rule applied to a BCS model for a variety of different normal-state scattering rates. The solid line is the conductivity sum rule applied to the $\epsilon_1(\omega; T > T_c)$ $N_n(\omega)$, while dashed line is for $\epsilon_1(\omega; T = T_c)$ $N_s(\omega)$; the dashed line is the difference between the two. The curves have been normalized to the full weight of the condensate ω_s to yield a dimensionless ratio. (a) $\Gamma = 2\Delta$, (b) $\Gamma = 2\Delta$, and (c) $\Gamma = 10\Delta$. The spectral weight transferred from the normal state to the condensate decreases with increasing Γ , illustrating the trend from the clean to dirty-limit case. Even for the largest value of Γ chosen, a large fraction of the condensate is captured by the integral at 2Δ .

be observed that nearly all of the spectral weight in the normal state collapses into the condensate. Furthermore, the condensate is essentially fully-formed above 2Δ . In Fig. 4(b) the normal-state scattering rate has been chosen to have an intermediate value $\Gamma = 2\Delta$ [the situation depicted in Fig. 2(b)]. The larger value of Γ has the effect of shifting more of the normal-state spectral weight above 2Δ , which reduces the strength of the condensate. This effect can be seen clearly in the sense that the dashed line which represents the strength of the condensate now falls well below the normal-state value. However, despite the larger value for Γ and the reduced strength of the condensate, it is once again almost fully-formed by 2Δ . Finally, in Fig. 4(c) a large normal-state scattering rate $\Gamma = 10\Delta$ is chosen to put the system into the dirty limit. The large scattering rate broadens the normal-state conduc-

tivity and moves a considerable amount of the spectral weight to high frequency, thus a relatively small amount of the spectral weight is transferred to the condensate. As the previous examination of the conductivity sum rule in Fig. 1 illustrated, to estimate ω_p^2 the cut-off frequency for the integral would have to be rather large. This contrasts with the formation of the condensate; by 2 almost 60% of the condensate has been captured, and by 4 the condensate is almost fully formed. This suggests that the relevant energy scale for the cut-off frequency for the integral for the condensate is close to 2, rather than the normal-state scattering rate which sets the scale for ω_p . This is an important result to which we will return to later.

B. $\text{YBa}_2\text{Cu}_3\text{O}_{6+x}$

The temperature dependence of the optical conductivity of optimally-doped $\text{YBa}_2\text{Cu}_3\text{O}_{6.95}$ ($T_c \approx 91$ K) for light polarized along the a axis is shown in Fig. 5(a). This sample contains a small amount of Ni (Cu_1_xNi_x , with $x = 0.0075$), which has the effect of lowering T_c by 2 K, but since the Ni appears to dope into the chains, the copper-oxygen planes remain unaffected.³¹ The Drude-like conductivity narrows as the temperature decreases from room temperature to just above T_c ; well below the superconducting transition the low-frequency conductivity has decreased and the missing spectral weight has collapsed into the condensate. It has been noted in the past that the conductivity is poorly described by the Drude model, and as a result a generalized form of the Drude model was adopted where the scattering rate was allowed to have a frequency dependence³⁵ (in order to preserve the Kramers-Kronig relation, the effective mass must also then have a frequency dependence). The frequency-dependent scattering rate has the form³⁶

$$\frac{1}{\tau(\omega)} = \frac{\omega_p^2}{4} \text{Re} \frac{1}{\omega(\omega)} : \quad (5)$$

The value for the plasma frequency used to scale the expression in Eq. (5) has been estimated using the conductivity sum rule for $\omega_p(\omega; T \neq T_c)$, using $\omega_c \approx 1$ eV, which yields a value for $\omega_{p,a} \approx 16700 \text{ cm}^{-1}$, or about 2 eV (Ref. 31). The frequency-dependent scattering rate $\tau_a(\omega)$ is shown in the inset of Fig. 5(a), and in the normal state shows a monotonic increase with frequency, and an overall downward shift with decreasing temperature. Below T_c , there is a strong suppression of $\tau_a(\omega)$ at low frequency, with a slight overshoot and then the recovery of the normal-state value at high-frequency. This behavior is characteristic of optimally-doped and overdoped materials.

The behavior of the oxygen-underdoped material $\text{YBa}_2\text{Cu}_3\text{O}_{6.60}$ ($T_c \approx 57$ K) for light polarized along the a axis, shown in Fig. 5(b), shows some significant differences from the optimally-doped material. The conductivity at room temperature is extremely broad. However,

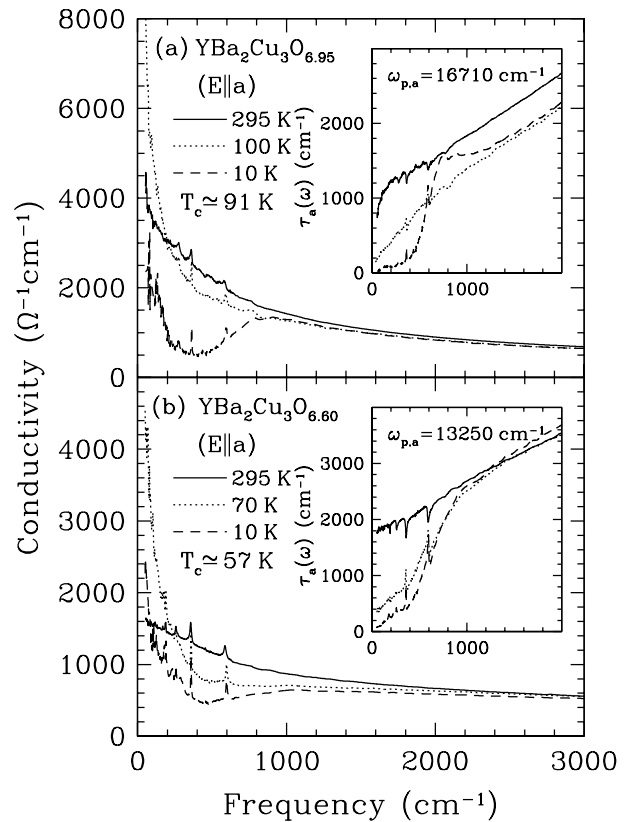


FIG. 5: The optical conductivity of (a) optimally-doped $\text{YBa}_2\text{Cu}_3\text{O}_{6.95}$, and (b) underdoped $\text{YBa}_2\text{Cu}_3\text{O}_{6.60}$ at room temperature (solid line), $T > T_c$ (dotted line), and $T < T_c$ (dashed line) for light polarized along the a axis. The inset in each panel shows the frequency dependent scattering rate and the estimated value of $\omega_{p,a}$. Each of these materials has a small Cu_1_xNi_x impurity ($x = 0.0075$) which lowers T_c somewhat and has implications for the CuO chains, but which otherwise leaves the CuO_2 planes unaffected. The Drude-like conductivity of the optimally-doped material narrows somewhat in the normal state but the scattering rate shows no indication of a pseudogap; below T_c a considerable amount of spectral weight collapses into the condensate. In the underdoped material, the conductivity narrows considerably in the normal state and the scattering rate indicates the opening of a pseudogap; the condensation is less dramatic than in the optimally-doped case.

at $T \neq T_c$ the conductivity has narrowed dramatically, and there has been a significant shift of spectral weight to the low frequency. For $T < T_c$ the low frequency conductivity has decreased, indicating the formation of a condensate, but the effect is not as dramatic as it was in the optimally-doped material, indicating that the strength of the condensate is not as great. The frequency-dependent scattering rate is shown in the inset, along with the estimated value of $\omega_{p,a} \approx 13250 \text{ cm}^{-1}$. As the temperature decreases in the normal state $\tau_a(\omega)$ decreases rapidly at low frequency, which is taken to be evidence for the formation of a pseudogap.^{19,36} The large drop in the scattering rate for $\omega \approx 0$ is a reflection of the dramatic

narrowing of the conductivity and is an indication that the reduced doping has not created a large amount of scattering due to disorder | on this basis, the system is not in the dirty limit.

The superfluid density $s_{s,a}$ has been estimated from the response of $\mathcal{I}^2_{1,a}(\omega)$ in the zero-frequency limit for $T = T_c$ for the optimally and underdoped materials, shown in Fig. 6. The estimate of s assumes that the response of $\mathcal{I}^2_{1,a}(\omega)$ at low frequency is dominated by the condensate, but it has been shown that along the c axis, there is enough residual conductivity to affect $\mathcal{I}^2_{1,c}(\omega)$ and thus the values of $s_{s,c}$, typically resulting in an overestimate of the strength of the condensate.^{37,38} The presence of residual conductivity for $T = T_c$ suggests that $s_{s,a}$ may be overestimated in this case as well. However, as we noted earlier, the real part of the conductivity in the superconducting state may be expressed as a regular part due to unpaired carriers, and a function at zero frequency; the frequency-dependent response to the function is manifested in the imaginary part of the conductivity. In the same way, the real part of the dielectric function is related to the strength of the condensate through the simple relation $\mathcal{I}^2_{1,a}(\omega) = \mathcal{I}^2_{1,a}(\omega_{ps}) = \mathcal{I}^2_{1,a}(\omega)$; this assumes no regular part of the real part of the dielectric function, and the response of the imaginary part is limited to the function, which is zero elsewhere. However, $\mathcal{I}^2_{2,a}(\omega)$ has been determined experimentally to be non-zero: if we refer to this as $\mathcal{I}^2_{2,a}(\omega)$, then $\mathcal{I}^2_{1,a}(\omega)$ may be determined through the Kramers-Kronig relation, and the superfluid density estimated as³⁸

$$s_{s,a}(\omega) = \mathcal{I}^2_{1,a}(\omega) - \mathcal{I}^2_{2,a}(\omega); \quad (6)$$

which should be a constant. This is shown in Fig. 6 at low frequency as the dotted lines. This method of estimating $s_{s,a}$ agrees well with the extrapolated values of $\mathcal{I}^2_{1,a}(\omega)$ for $\omega = 0$ and indicates that if there is a correction associated with the residual conductivity for $T = T_c$, then it is quite small. The estimated values for the condensate are $s_{s,a}^{1=2} = 8670 \text{ cm}^{-1}$ and 5620 cm^{-1} for the optimally and underdoped materials, respectively; these estimates are in good agreement with previous estimates.³¹ In both materials there is a slight suppression of $\mathcal{I}^2_{1,a}(\omega)$ in the $500 - 700 \text{ cm}^{-1}$ region, which is in agreement with estimates for the superconducting gap maximum $2\Delta_0 \approx 500 \text{ cm}^{-1}$ (adopting the notation for a d-wave superconductor) in overdoped $\text{YBa}_2\text{Cu}_3\text{O}_{6.99}$ (Ref. 39). Studies of other cuprate systems suggest that the gap maximum increases with decreasing doping,^{13,40,41} despite the reduction of T_c .

The integrated values of the conductivity in the normal ($T > T_c$) and superconducting ($T = T_c$) states are indicated by the solid [$N_n(\omega)$] and dashed [$N_s(\omega)$] lines for $\text{YBa}_2\text{Cu}_3\text{O}_{6.95}$ and $\text{YBa}_2\text{Cu}_3\text{O}_{6.60}$ along the a axis in the upper and lower panels of Fig. 7, respectively. For $\text{YBa}_2\text{Cu}_3\text{O}_{6.95}$, $N_n(\omega)$ increases rapidly with frequency, but does not display any unusual structure. On the other hand, $N_s(\omega)$ evolves more slowly, and has several injection points at low frequency which are thought to

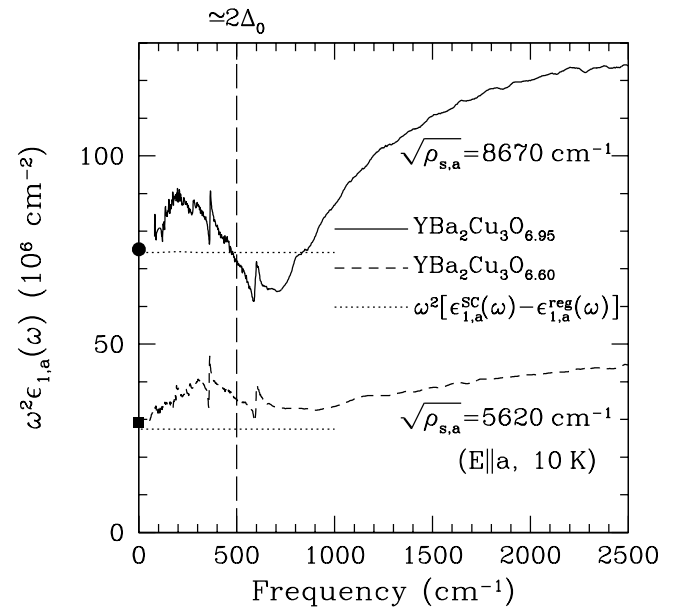


FIG. 6: The function $\mathcal{I}^2_{1,a}(\omega)$ vs frequency for optimally doped $\text{YBa}_2\text{Cu}_3\text{O}_{6.95}$ (solid line) and underdoped $\text{YBa}_2\text{Cu}_3\text{O}_{6.60}$ (dashed line) along the a axis at $T = 10 \text{ K}$ (T_c). The superfluid density is $s = \mathcal{I}^2_{1,a}(\omega = 0)$; taking the squares to render the units the same as those of a plasma frequency yields $\sqrt{p_{s,a}} = 8670 \text{ cm}^{-1}$ and $\sqrt{p_{s,a}} = 5620 \text{ cm}^{-1}$ for the optimally and underdoped materials, respectively. Note also that in both materials there is a slight suppression of $\mathcal{I}^2_{1,a}(\omega)$ in the $500 - 700 \text{ cm}^{-1}$ region, close to the estimated value of $2\Delta_0$.

be related to the spectral function.⁴² The difference between the two curves $\mathcal{I}^2_{ps} = N_n(\omega) - N_s(\omega)$ is shown by the dashed line in Fig. 7(a). This quantity increases quickly and then saturates above 800 cm^{-1} to a constant value. This plot is reminiscent of the BCS dirty limit case discussed in Fig. 2(c). The sum rules applied to $\text{YBa}_2\text{Cu}_3\text{O}_{6.60}$ shown in Fig. 7(b) are similar to the optimally-doped case except that the overall magnitude has decreased, a reflection of the decreased carrier concentration within the copper-oxygen planes in the underdoped material. While the condensate is also lower, it now appears that it does not saturate as quickly as was the case in the optimally-doped material.

A more detailed examination of the evolution of the weight of the condensate for $\text{YBa}_2\text{Cu}_3\text{O}_{6.95}$ (solid line) and $\text{YBa}_2\text{Cu}_3\text{O}_{6.60}$ (dotted line), normalized to the values of $s_{s,a}$ determined in Fig. 6, is shown in Fig. 8. When the FG T sum rule is exhausted, the ratio is unity by definition. For the optimally-doped material, this occurs rapidly and the ratio approaches unity at $\omega_c \approx 800 \text{ cm}^{-1}$. About 80% of the spectral weight in the underdoped material has also formed 800 cm^{-1} , but the remaining 20% of the spectral weight is only recovered at much higher frequencies ($\omega_c \approx 5000 \text{ cm}^{-1}$); there is also some evidence for an injection point near 800 cm^{-1} , indicating that at some level there is a common energy scale in the

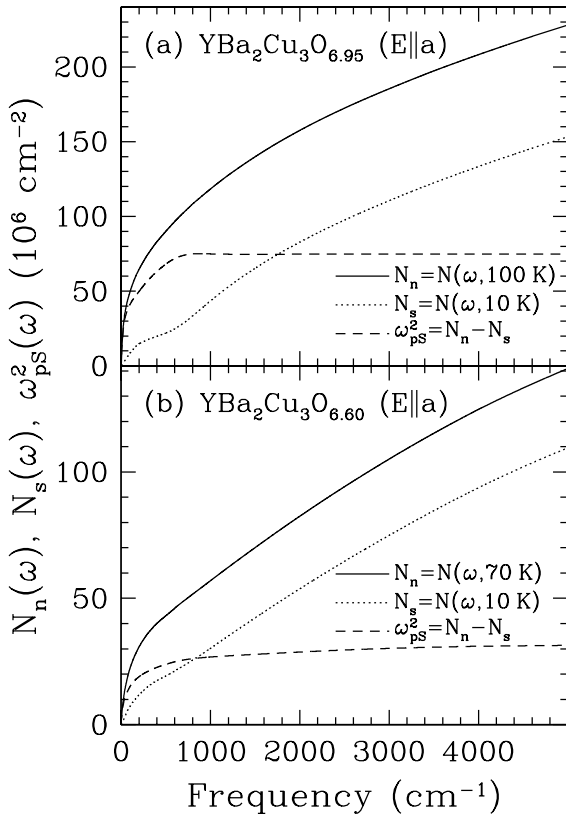


FIG . 7: The conductivity sum rules applied to (a) optimally-doped $\text{YBa}_2\text{Cu}_3\text{O}_{6.95}$ and (b) underdoped $\text{YBa}_2\text{Cu}_3\text{O}_{6.60}$ for light polarized along the a axis for $T > T_c$ [N_n (!), solid line] and for $T = T_c$ [N_s (!), dotted line]; the difference is the estimate of the strength of the condensate from the Ferrell-Glover-Tinkham sum rule (dashed line). The condensate saturates in the upper panel by $\sim 800 \text{ cm}^{-1}$, while in the lower panel the frequency at which the full weight of the condensate is recovered seems to be much higher. In the upper panel the magnitudes of the curves are greater than in the lower panel; a reflection of the decreased carrier concentration.

two systems. It is tempting to draw an analogy with the BCS dirty-limit case and argue that the spectral weight in the underdoped material has been pushed to higher frequency in response to an increase in the normal-state scattering. However, there are two important points that argue against this interpretation. First, an examination of scattering rate in the insets of Fig. 5 for $T > T_c$ indicates that the $1 = a (! ! 0) < 200 \text{ cm}^{-1}$ for both materials.

Second, if the conductivity is fitted using a Drude-Lorentz model [i.e., the Drude model shown in Eq. (2) with some bound excitations] then the nature of the low-frequency conductivity places hard constraints on the width of the Drude peak,⁴³ $\sim 140 \text{ cm}^{-1}$ for optimally-doped $\text{YBa}_2\text{Cu}_3\text{O}_{6.95}$, and $\sim 100 \text{ cm}^{-1}$ for underdoped $\text{YBa}_2\text{Cu}_3\text{O}_{6.60}$. In every case, $\sim 2 \text{ eV}$, indicating that while ω has an unusual temperature dependence, these materials are not in the dirty limit. In addition, just

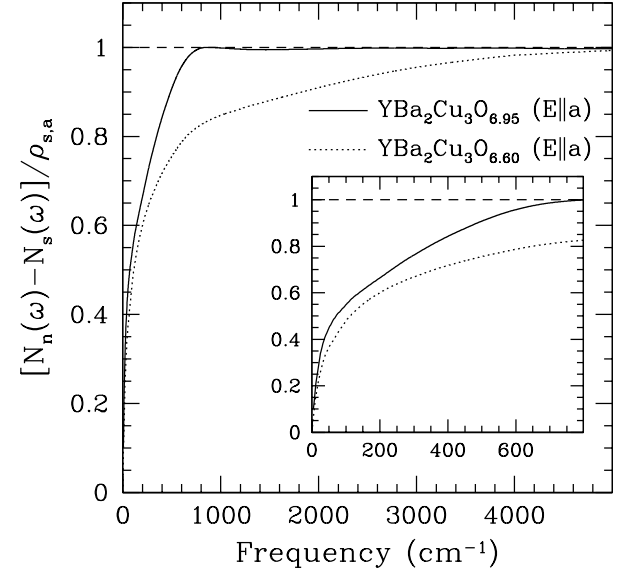


FIG . 8: The normalized weight of the condensate N_n (!) N_s (!) = $\rho_{s,a}$ for optimally-doped $\text{YBa}_2\text{Cu}_3\text{O}_{6.95}$ (solid line) and underdoped $\text{YBa}_2\text{Cu}_3\text{O}_{6.60}$ (dotted line) along the a axis direction. The curves describing the condensate have been normalized to the values of $\rho_{s,a}$ shown in Fig. 6. The condensate for the optimally-doped material has saturated by $\sim 800 \text{ cm}^{-1}$, while in the underdoped material the condensate is roughly 80% formed by this frequency, but the other 20% is not recovered until much higher frequencies. Inset: The low-frequency region.

above T_c the scattering rate has actually decreased in the underdoped material, indicating that there is less normal-state scattering at low temperature ($T > T_c$). Thus, the larger energy scale in the underdoped system has a different origin. The two very different types of behavior observed in the optimally and underdoped materials suggests that the behavior of the electronic correlations in the normal state determine the nature of the superconductivity in these materials²² and the degree to which the kinetic energy may play a role.

C. Kinetic energy arguments

The unconventional nature of the superconductivity in the cuprate systems has led to the suggestion that the contribution of the kinetic energy to the condensation energy is not negligible.⁷ In such a case the FG T sum rule must be modified to take on the form⁸

$$s_{pr} = \frac{120}{\int_{0+}^{Z_{!c}} [A_{1,r} (! ; T' - T_c) - A_{1,r} (! ; T - T_c)] d!} + \frac{e^2 a_r^2}{2h^2 V_m} [h \cdot T_{1,r} - T_c - h \cdot T_{1,r} - T_c]; \quad (7)$$

$$A_{1,r} + A_{h,r};$$

where a is the lattice spacing, V_m is the size of the unit cell, and T_r is that part of the kinetic energy along the r direction associated with the carriers in the valence band (or hopping processes in the case where the transport is incoherent, i.e. along the c axis).^{8,9} The low-frequency term $A_{1,r}$ corresponds to the FGT sum rule, while $A_{h,r}$ corresponds to the high-frequency part of the integral, which is in fact the kinetic energy contribution. In a conventional BCS superconductor where λ_c is of the order 2, $A_{h,r} = 0$ and the FGT sum rule holds, thus $s_{1,a} = A_{1,a}$. In a system where the kinetic energy plays a prominent role then $A_{h,r} \neq 0$ and the FGT sum rule will appear to be violated. However, as Fig. 8 indicates, the FGT sum rule holds for the optimally-doped materials and is exhausted at energies of the order of the maximum of the superconducting energy gap. The FGT sum rule is also obeyed for the underdoped material as well, but the frequency range required to capture the full spectral weight of the condensate is now much greater than the energy scale associated with the formation of a superconducting energy gap (of the order of 0.6 eV). Thus, it would appear that the contribution of the kinetic energy to the condensation energy is at or below the limit of the experimental error, or roughly 0.5%. However, if the normal state is not described by a Fermi liquid, then the distinction between potential and kinetic energy becomes somewhat cloudy.²⁷ The unusual energetics of the underdoped material is also observed in the behavior of the optical conductivity along the c axis.

D. Sum rules along the c axis

The optical properties of $\text{YBa}_2\text{Cu}_3\text{O}_{6+x}$ have been examined in some detail along c axis,^{20,44,45,46} where both the optical conductivity and the strength of the condensate are much lower than the highly-conducting a - b planes. The optical conductivity (especially in the more underdoped materials) is dominated by the un-screened phonons.^{47,48} Given that large changes in the phonon spectrum have been observed at low temperature in the underdoped materials,^{20,49,50,51} the application of the FGT sum rule must be treated with some care; in the studies cited here,^{16,18} the integral has been truncated at

800 cm^{-1} . The application of the FGT sum rule along the c axis has shown that while this sum rule is not violated in the optimally-doped materials, as these materials become increasing underdoped and a pseudogap has formed, the FGT sum rule is violated. For $\text{YBa}_2\text{Cu}_3\text{O}_{6.60}$ more than 50% of the c -axis spectral weight is missing at low temperature.^{16,18} The violation of the FGT sum rule has been proposed as evidence for a kinetic energy contribution to $s_{c,c}$, although there have also been other interpretations of this phenomena.⁵² The implication is that the missing spectral weight is recovered at high frequency, but it is unclear at precisely what point this occurs.

The observation that the FGT sum rule is obeyed

in the optimally-doped materials for energies of the order 20 in the copper-oxygen planes and along the c axis is similar to the BCS model and suggests that any contribution of the kinetic energy to s_c is not detectable within the sensitivity of this experiment. In the underdoped materials the FGT sum rule is violated along the c axis.¹⁸ Although the FGT sum rule is not violated in the copper-oxygen planes, the frequency range required to exhaust the sum rule has increased dramatically from $\lambda_c \approx 800 \text{ cm}^{-1}$ to $> 5000 \text{ cm}^{-1}$. The condensate is also not recovered as quickly at low frequency; while 90% of the spectral weight in the optimally-doped material has been recovered by 500 cm^{-1} , the same value has not been reached in the underdoped material until $> 1800 \text{ cm}^{-1}$, as shown in Fig. 8.

The conductivity along the c axis is thought to be incoherent, indicating that the transport properties perpendicular to the copper-oxygen planes arise from the density of states within the planes. It has been suggested that the c -axis properties are particularly sensitive to the $(0; \pi)$ part of the Fermi surface where the superconducting gap is observed to open at T_c (as well as the pseudogap in the underdoped materials below T_c). This connection between the a - b planes and the c axis suggests that if the FGT sum rule along the c axis were extended to $\lambda_c \approx 5000 \text{ cm}^{-1}$ then the spectral weight would be recovered and the c axis sum rule would yield $s_{c,c}$. However, the general consensus at this time is that the conductivity data is not yet sufficiently precise along the c axis to confirm this prediction.

E. Potential and kinetic energy

If the violation of the FGT sum rule in the underdoped material along the c axis is due to a kinetic energy contribution to the condensate, then a similar violation might also be observed in the copper-oxygen planes. The fact that this is not the case may be attributed to one of several things: (i) the relative contribution to s_c is too small to be observed, or (ii) the kinetic and potential energy are mixed,²⁷ preventing a simple test such as the FGT sum rule from distinguishing between the two.

The rapid convergence of s_c in the optimally-doped material is what would be expected in a BCS system in which the normal state is a Fermi liquid and the condensation is driven by the potential energy. While none of the cuprate superconductors are truly good metals, it has been suggested that for $T > T_c$ the overdoped materials may resemble a Fermi liquid,⁵³ implying that the potential rather than kinetic energy drives the transition. On the other hand, it is recognized that the underdoped materials are "bad metals" and exhibit non-Fermi liquid behavior. However, if the upper limit for the FGT sum rule is extended then there is no violation. This would tend to argue against any substantial contribution of the kinetic energy to the condensate, in agreement with other studies of underdoped systems.²⁴ However,

the suggestion that the potential and kinetic energy may be fixed in underdoped materials makes it to distinguish between the two. It is tempting to view the crossover in the rate of convergence in the condensate in Fig. 8 for the underdoped material as a line of demarcation; below

800 cm⁻¹, or of the order 2⁰, the integral captures one type of behavior and that above this point another is represented. In theory this might allow for a kinetic energy contribution to σ that is larger than previously suggested, but in practice no definitive statement can be made.

IV. CONCLUSIONS

The optical conductivity sum rule has been examined for the Drude model, and the normal state scattering rate has been determined to be the relevant energy scale ($\epsilon_c \approx 8$) to recover σ_p . The Ferrell-Glover-Tinkham sum rule has been applied to the BCS model where the relevant energy scale to recover the strength of the condensate σ_s is the superconducting energy gap ($\epsilon_c \approx 2$, slightly larger in the extreme dirty-limit case); there is only a weak dependence on ϵ_c .

The FGT sum rule has been examined for light polar-

ized along the a axis direction in the high-temperature superconductors $YBa_2Cu_3O_{6.95}$ and $YBa_2Cu_3O_{6.60}$. The FGT sum rule is obeyed in both materials. The energy scale required to recover the full strength of the condensate in the optimally doped material is $\epsilon_c \approx 800$ cm⁻¹ (≈ 2), in good agreement with the estimates from the BCS model. However, the energy scale in the underdoped materials is much higher, $\epsilon_c \approx 5000$ cm⁻¹. This effect can not be attributed to increased scattering, as $\sigma \propto \epsilon_c^2$ in both materials. The two very different types of behavior observed in the optimal and underdoped materials suggests that the behavior of the electronic correlations in the normal state determine the nature of the superconductivity in these materials²² and the degree to which the kinetic energy may play a role.

Acknowledgments

We would like to thank D.N. Basov, V.J. Emery, A. Chubukov, S.A. Kivelson, D. van der Marel, F.M. Marsiglio, C. Pepin, M. Strongin, D.B. Tanner, T.Timusk, J.M. Tranquada, and J.J. Tu for useful discussions. This work was supported by the Department of Energy under contract number DE-AC02-98CH10886.

Electronic address: homes@bnl.gov

- ¹ D.Y. Smith, in *Handbook of Optical Constants of Solids*, edited by E.D. Palik (Academic, New York, 1985), pp. 35-68.
- ² R.A. Ferrell and R.E. Glover, III, *Phys. Rev.* **109**, 1398 (1958).
- ³ M. Tinkham and R.A. Ferrell, *Phys. Rev. Lett.* **2**, 331 (1959).
- ⁴ J. Bardeen, L.N. Cooper, and J.R. Schrieffer, *Phys. Rev.* **108**, 1175 (1957).
- ⁵ M. Tinkham, *Introduction to Superconductivity* (McGraw-Hill, New York, 1966).
- ⁶ S. Chakravarty, *Eur. Phys. J. B* **5**, 337 (1998).
- ⁷ J. Hirsch, *Physica C* **199**, 305 (1992).
- ⁸ J.E. Hirsch and F.M. Marsiglio, *Phys. Rev. B* **62**, 15131 (2000).
- ⁹ J.E. Hirsch and F.M. Marsiglio, *Physica C* **331**, 150 (2000).
- ¹⁰ M.R. Norman, M.Randeria, B.Janko, and J.C. Campuzano, *Phys. Rev. B* **61**, 14742 (2000).
- ¹¹ R. Haslinger and A.V. Chubukov (2002), cond-mat/0209600.
- ¹² P.A. Lee, *Physica C* **317**, 194 (1999).
- ¹³ P.W. Anderson, *Physica C* **341**-348, 9 (2000).
- ¹⁴ V.J. Emery and S.A. Kivelson, *J. Phys. Chem. Solids* **61**, 467 (2000).
- ¹⁵ S. Alexiev and N.F. Mott, *High Temperature Superconductors and Other Superfluids* (Taylor and Francis, London, 1994).
- ¹⁶ D.N. Basov, S.I. Woods, A.S. Katz, E.J. Singley, R.C. Dynes, M.Xu, D.G. Hinks, C.C. Homes, and M. Strongin, *Science* **283**, 49 (1999).
- ¹⁷ M.V. Klein and G. Blumberg, *Science* **283**, 42 (1999).
- ¹⁸ D.N. Basov, C.C. Homes, E.J. Singley, M. Strongin, T.Timusk, G. Blumberg, and D. van der Marel, *Phys. Rev. B* **63**, 134514 (2001).
- ¹⁹ T.Timusk and B. Statt, *Rep. Prog. Phys.* **62**, 61 (1999).
- ²⁰ C.C. Homes, T.Timusk, D.A. Bonn, R. Liang, and W.N. Hardy, *Phys. Rev. Lett.* **71**, 1645 (1993).
- ²¹ A.A. Tsvetkov, D. van der Marel, K.A.M. Oler, J.R. Kirtley, J.L.D. Boer, A.M. Eetstra, Z.F. Ren, N.K. Oleshnikov, D. Duletic, A. Damascelli, et al., *Nature* **395**, 360 (1998).
- ²² M.R. Norman and C. Pepin, *Phys. Rev. B* **66**, 100506 (2002).
- ²³ D. van der Marel (private communication).
- ²⁴ H.J.A.M. Olegraaf, C.P. Resura, D. van der Marel, and P.H.K. Adn M. Li, *Science* **295**, 2239 (2002).
- ²⁵ A.F. Santander-Syro, R.P.S.M. Lobo, N. Bontemps, Z. Kostantinovic, Z. Li, and H. Ray, *Phys. Rev. Lett.* **88**, 097005 (2002).
- ²⁶ A.F. Santander-Syro, R.P.S.M. Lobo, N. Bontemps, Z. Kostantinovic, Z. Z. Li, and H. Ray (2001), cond-mat/0111539.
- ²⁷ S. Chakravarty, H.-Y. Kee, and E. Abraham (2002), cond-mat/0211613.
- ²⁸ R. Liang, P. Dusanjin, D.A. Bonn, D.J. Baar, J.F. Carolan, and W.N. Hardy, *Physica C* **195**, 51 (1992).
- ²⁹ P. Schlegel, W.N. Hardy, and B.X. Yang, *Physica C* **176**, 261 (1991).
- ³⁰ C.C. Homes, M. Reedyk, D.C. Randles, and T.Timusk, *Appl. Opt.* **32**, 2972 (1993).
- ³¹ C.C. Homes, D.A. Bonn, R. Liang, W.N. Hardy, D.N. Basov, T.Timusk, and B.P. Clayman, *Phys. Rev. B* **60**, 9782 (1999).
- ³² The term 120= before the integral assumes that the units

of conductivity are in cm^{-1} , so that the integral yields cm^{-2} . The factor in front of the integral is sometimes expressed as $2m/V_c = e^2$, where V_c is the volume of the unit cell, in which case the integral yields the effective number of carriers.

³³ V. J. Emery, S. A. Kivelson, and O. Zachar, *Phys. Rev. B* **56**, 6120 (1997).

³⁴ W. Zimermann, E. H. Brandt, M. Bauer, E. Seider, and L. Genzel, *Physica C* **183**, 99 (1991).

³⁵ B. C. Webb, A. J. Sievers, and T. M. Thalissin, *Phys. Rev. Lett.* **57**, 1951 (1986).

³⁶ A. V. Puchkov, D. N. Basov, and T. Timusk, *J. Phys.: Condens. Matter* **8**, 10049 (1996).

³⁷ C. C. Homes, S. Kamal, D. A. Bonn, R. Liang, W. N. Hardy, and B. P. Clayman, *Physica C* **296**, 230 (1998).

³⁸ S. V. Dordevic, E. J. Singley, D. N. Basov, S. Komiyama, Y. Ando, E. Bucher, C. C. Homes, and M. Strongin, *Phys. Rev. B* **65**, 124511 (2002).

³⁹ D. H. Lu, D. L. F. Adn N. P. Armistage, K. M. Shen, A. Damascelli, C. Kim, F. Ronning, Z.-X. Shen, D. A. Bonn, R. Liang, W. N. Hardy, et al., *Phys. Rev. Lett.* **86**, 4370 (2001).

⁴⁰ J. M. Harris, Z.-X. Shen, P. J. Whittle, D. S. Marshall, M. C. Schabel, J. N. Eckstein, and I. Bozovic, *Phys. Rev. B* **54**, R15665 (1996).

⁴¹ N. Miyakawa, J. F. Zasadzinski, L. Ozyuzer, P. Gupatasamai, D. G. Hinks, C. Kendziora, and K. E. Gray, *Phys. Rev. Lett.* **83**, 1018 (1999).

⁴² J. J. Tu, C. C. Homes, G. D. Gu, D. N. Basov, and M. Strongin, *Phys. Rev. B* **66**, 144514 (2002).

⁴³ M. A. Quijada, D. B. Tanner, R. J. Kelley, M. Onellion, H. Berger, and G. M. Margaritondo, *Phys. Rev. B* **60**, 14917 (1999).

⁴⁴ J. Schutmann, S. Tajima, S. Miyamoto, and S. Tanaka, *Phys. Rev. Lett.* **73**, 174 (1994).

⁴⁵ C. C. Homes, T. Timusk, D. A. Bonn, R. Liang, and W. N. Hardy, *Physica C* **254**, 265 (1995).

⁴⁶ S. Tajima, J. Schutmann, S. Miyamoto, I. Terasaki, Y. Sato, and R. Hau, *Phys. Rev. B* **55**, 6051 (1997).

⁴⁷ C. C. Homes, T. Timusk, D. A. Bonn, R. Liang, and W. N. Hardy, *Can. J. Phys.* **73**, 663 (1995).

⁴⁸ J. Schutmann, S. Tajima, S. Miyamoto, Y. Sato, and R. Hau, *Phys. Rev. B* **52**, 13665 (1995).

⁴⁹ D. Munzar, C. Bernhard, A. Golnik, J. Humilcek, and M. Cardona, *Solid State Commun.* **112**, 365 (1999).

⁵⁰ M. Gminger, D. van der Marel, A. A. Tsvetkov, and A. Erb, *Phys. Rev. Lett.* **84**, 1575 (2000).

⁵¹ C. Bernhard, D. Munzar, A. Golnik, C. T. Lin, A. W.ittlin, J. Humilcek, and M. Cardona, *Phys. Rev. B* **61**, 618 (2000).

⁵² L. B. Ioffe and A. J. Millis, *Science* **285**, 1241 (1999).

⁵³ C. Proust, E. Boaknin, R. W. Hill, L. Taillefer, and A. P. Mackenzie, *Phys. Rev. Lett.* **89**, 147003 (2002).